Available online at ScienceDirect www.sciencedirect.com
Elsevier Masson France EM|consulte www.em-consulte.com
BIOMEDICINE & PHARMACOTHERAPY
Biomedicine & Pharmacotherapy 63 (2009) 155–164

Original article

Meso-tetra (carboxyphenyl) porphyrin (TCPP) nanoparticles were internalized by SW480 cells by a clathrin-mediated endocytosis pathway to induce high photocytotoxicity

Zhiyuan Hu, Yifeng Pan, Jiwei Wang, Jiji Chen, Jing Li, Lifeng Ren*

Department of Biomedical Engineering, Xiangya School of medicine, Central South University, Changsha, Hunan 410078, China

Received 27 July 2007; accepted 23 July 2008
Available online 24 August 2008

Abstract

We studied the uptake of meso-tetra (carboxyphenyl) porphyrin (TCPP) nanoparticles by SW480 cells and carried out a systematic investigation of the cellular internalization mechanism of TCPP nanoparticles, also studied the photocytotoxicity of TCPP nanoparticles. At first, meso-tetra (carboxyphenyl) porphyrin (TCPP) nanoparticles were prepared by the method of mixing solvent techniques. SW480 cellular uptakes of photosensitizers (TCPP nanoparticles, TCPP-loaded poly (lactic-co-glycolic acid) (PLGA) nanoparticles and free TCPP) were analyzed by the method of fluorospectrophotometry. Endocytosis mechanism investigation was carried out by preincubating SW480 cells at 4 °C, and preincubating SW480 cells with sucrose, K^+-free buffer solution and filipin. Clathrin HC expression after incubating SW480 cells with these three photosensitizers was analyzed by methods of Western blot and RT-PCR. At last, we analyzed the photo-cytotoxicity after incubating SW480 cells with photosensitizers and receiving irradiation. SW480 cells showed rapid uptake (0.0083 fmoles TCPP/cell) of TCPP nanoparticles after 1 h incubation. We also demonstrated that the uptake of TCPP nanoparticles by SW480 cells was a clathrin-mediated endocytosis pathway. As a result of rapid internalization of TCPP nanoparticles by SW480 cells, this special photosensitizer showed very high photocytotoxic effect on SW480 cells *in vitro*. The nano-sized photosensitizer with no matrix cover: TCPP nanoparticles, can produce higher photocytotoxicity than other photosensitizers (TCPP-loaded PLGA nanoparticles and free TCPP). The *in vivo* tumor growth inhibition experiment indicated that TCPP nanoparticles plus PDT treatment induced the most dramatic tumor-inhibiting efficacy in all TCPP treated groups. The results of this study suggest that TCPP nanoparticles represent a potential and powerful photodynamic therapy agent.

Keywords: Meso-tetra (carboxyphenyl) porphyrin; Nanoparticles; Photodynamic therapy; Endocytosis; Clathrin; SW 480 cells

1. Introduction

Photodynamic therapy (PDT) is the combination of light and light sensitive agents (such as porphyrins) in an oxygen-rich environment. PDT has been beneficial in the treatment of cancer, such as choroidal neovascularization due to age-related macular degeneration [1], ovarian cancer [2] and oral pre-cancer [3].

Hydrophobic nature of many photosensitizers results in two inevitable problems: the delivery in blood circulation and the low photo-physical properties due to the aggregation of photosensitizers, decreasing the photo-oxidation efficacy to achieve the photodynamic therapy. This main property makes necessary to obtain suitable pharmaceutical formulations. Suitable carrier and delivery systems for photosensitizers should have a simple but effective strategy to realize high selectivity, high photodynamic efficacy and should have low side effects [4]. A variety of delivery systems have been studied, such as polymer carriers [5], liposomes [6,7], and bioconjugates [8–10]. In these strategies, photosensitizers are

Abbreviations: TCPP, meso-tetra (carboxyphenyl) porphyrin; PDT, photodynamic therapy; PLGA, poly (lactic-co-glycolic acid); PEG, polyetheylene glycol; CHC, clathrin heavy chains; HC, heavy chains; RT-PCR, reverse transcription-polymerase chain reaction; FCS, fetal calf serum; DMEM, Dulbecco's modified Eagle's medium; SEM, scanning electron micrograph.

* Corresponding author.
E-mail address: plapeorgd@yahoo.com.cn (L. Ren).

0753-3322/$ - see front matter © 2008 Elsevier Masson SAS. All rights reserved.
doi:10.1016/j.biopha.2008.07.087

either encapsulated into external matrix or conjugated with peptide by intermolecular interaction. Photosensitizers encapsulated in carries can't interact with cells directly after accumulate in targeted tissue, they must make function after release from matrix. Photosensitizers binding with targeted molecule don't have nanoscale special properties of nanomaterials, such as great surface area. Porphyrin loaded polymer nanometer carriers prepared by using Tween 80 have shown better drug loading ratio and improved tumor uptake over free drugs [11,12]. But such emulsifying agents could lead to acute hypersensibility reactions *in vivo* [13,14]. Liposomes encapsulating hydrophobic drugs suffer from poor drugs loading and increased self-aggregation of the drug in the entrapped state [15,16]. Liposomes are also prone to opsonization and subsequent capture by the major defense system of the body (reticuloendothelial system, or RES) [16]. Another major disadvantage, common to all of the above-mentioned delivery systems, which are based on controlled release of the photosensitive drugs, is the posttreatment accumulation of the free drugs in the skin and the eye, resulting in phototoxic side effects, which may last for at least a month [17]. Nanoscaled particles composed of porphyrins without coated with external matrix are expected to have chemical activities significantly different from those of the free porphyrins or of those encapsulated in matrix. These expected nanoparticles are promising components of advanced materials because of the rich photochemistry, stability, and proven catalytic activity.

Xianchang Gong et al. [18] reported the first synthesis and characterization of porphyrin nanoparticles that are neither self-assembled by designed intermolecular interactions nor encapsulated in an external matrix by using mixing solvent techniques.

Endocytosis is involved in an enormous variety of cellular processes. The many functions in which endocytosis plays a role, including antigen presentation, nutrient acquisition, clearance of apoptotic cells, pathogen entry, receptor regulation, hypertension, and synaptic transmission. The basic mechanisms underlying endocytosis have fascinated cell biologists for more than two decades, but it has become clear only recently how clathrin-coated vesicle budding from the plasma membrane is initiated at the molecular level [19].

Nanoparticles have been utilized to enhance the absorption of therapeutic drugs and genes [20,21]; information about the mechanism of the endocytic machinery involved, as well as about nanoparticles intracellular trafficking, is sparse [22]. Endocytosis of NPs may occur through various endocytic processes which have not been fully identified [23–25]. Qaddoumi and colleagues have shown that in primary cultures of rabbit conjunctival epithelial cells (RCEC), endocytosis of poly (DL-lactide-co-glycolide) (PLGA) NPs occurs mainly via clathrin- and caveolin-1-independent pathways [26]; these authors suggested that NP uptake occurs by adsorptive endocytosis [27]. Internalization of cationic chitosan NPs appears to occur predominantly by adsorptive endocytosis and in part by a clathrin-mediated process [23,28–31]. Stable 20–200 nm diameter porphyrin nanoparticles from *meso*-tetra (carboxyphenyl) porphyrin were prepared by a general method in our research. This stable porphyrin nanoparticles showed functionalization of the stabilizer for targeted cell delivery [32]. Understanding the molecular mechanisms that underlie the interactions of these porphyrin nanoparticles with the cell and their endocytic pathway is crucial for the successful development of these vehicles. In the present investigation, we performed a study on the mechanism of internalization of porphyrin nanoparticles by SW480 cells. We also investigated the uptake of porphyrin nanoparticles by SW480 cells. We show that greater internalization and accumulation of the nanoparticles in SW480 cells happen by the clathrin-mediated endocytic pathway. Greater accumulation of nanoparticles induces higher photocytotoxicity *in vitro* and higher *in vivo* tumor-inhibiting efficacy than other photosensitizers in our research.

2. Materials and methods

2.1. Materials

Meso-tetra (carboxyphenyl) porphyrin (TCPP), poly (DL-lactide-co-glycolide) (PLGA), Sucrose, polyvinyl alcohol (PVA) were purchased from Sigma-Aldrich (St. Louis, MO).

Filipin was purchased from SINOPHARM Co., Ltd (Beijing, China).

2.2. Cell lines

Human colon carcinoma cell lines: SW480 cells, HT-29 cells and LS174T cells were grown in Dulbecco's modified Eagle's medium (DMEM) without Phenol Red supplemented with 10% heat inactivated fetal bovine serum (FBS), 100 units/m penicillin and 100 μg/ml streptomycin (GIBCO® Life Technologies, CA). J774 cells were grown in Roswell Park Memorial Institute 1640 medium containing 10% heat inactivated FBS, 100 units/m penicillin and 100 g/ml streptomycin (GIBCO® Life Technologies, CA). All cells were cultured at 37 °C in 5% CO_2 atmosphere.

2.3. Preparation of meso-tetra (carboxyphenyl) porphyrin (TCPP) nanoparticles

Meso-tetra (carboxyphenyl) porphyrin (TCPP) nanoparticles were prepared by the method of Xianchang Gong described in former paper [18]. The procedure to prepare nanoparticles was: 1.9 mg meso-tetra (carboxyphenyl) porphyrin (TCPP) was dissolved in 4 ml DMSO to make a stock solution. 0.4 ml stock solution was transferred to a test tube followed by addition of 50 μl triethylene glycol monomerthylether. After 1 min, 5 ml water was added to this mixture and a glass rod was used to stir the mixture. The organic solvent DMSO was removed by rotary evaporation. Sterilization by filtering through a Steriflip® filter unit with 0.22 μm Millipore Express™ (Millipore®, Volketswill, Switzerland) was carried out. The mean particle size was assessed by photon correlation spectroscopy using a Zetasizer® 5000 (Malvern, Worcestershire, England). The surface morphology

of the nanoparticles was observed using a JEOL JSM-6360LV scanning electron microscope (SEM) at 20.0 kV. The samples were mounted onto stubs by means of quick drying silver paint, and then coated with gold palladium to a thickness of approximately 25 nm.

2.4. Preparation of TCPP-loaded PLGA nanoparticles

TCPP-loaded PLGA nanoparticles were prepared by the method described in former paper [33]. Briefly, 6 g of organic phase consisting of PLGA (500 mg) and TCPP (50 mg) dissolved in benzyl alcohol was emulsified with 8 g of aqueous solution of polyvinyl alcohol (PVA) (17% [m/m]). After 15 min of mechanical stirring at 2000 rpm, 500 ml of distilled water was added to the resulting emulsion to allow complete diffusion of the benzyl alcohol into the aqueous phase, leading to the formation of nanoparticles. The drug content and entrapment efficiency were determined spectrophotometrically at 416 nm by Hitach-4000 fluorescence spectrophotometer (Hitach, Japan).

2.5. Cellular uptake of photosensitizers

An appropriate number of SW480 cells were cultured in 25 cm^2 culture flasks at a density that the cells reached, and incubated to obtain nearly confluent cell layers after 3 days. Then the cells incubated with TCPP nanoparticles and TCPP-loaded PLGA nanoparticles by replacing the original 2 ml of media with 2–4 ml of media containing these PS. The final concentration of TCPP in each incubated solution was 1 μM. SW480 cells were treated with these three photosensitizers for 30 min, 1 h, 2 h and 3 h in the dark at 37 °C. In order to investigate the confirmative internalization mechanism of these three photosensitizers by colon cancer cells, we also compared the uptake of free TCPP, TCPP-loaded PLGA nanoparticles and TCPP nanoparticles in two additional colon cancer cells: HT-29 cells and LS174T cells. These cancerous cells were also treated with these three photosensitizers for 30 min, 1 h, 2 h and 3 h in the dark at 37 °C. J774 cells were incubated with these three photosensitizers for 3 h in the dark at 37 °C. Afterwards, the medium containing the PS was removed, the cells were washed three times with 2 ml of PBS. Cells were collected by using trypsin to form 1 ml cell suspensions in culture medium (without any FBS) for each dish. A 0.5 ml of 1 ml cell suspension was solubilized in 2 ml of 1 M NaOH-1% SDS in a fluorometer cuvette to quantitate the TCPP content in the solubilized cell suspension in Hitach-4000 fluorescence spectrophotometer (Hitach, Japan). The concentration of the porphyrin in sample was estimated by comparison with a calibration curve obtained with standard solutions of TCPP in 1% SDS. The remaining 0.5 ml of each cell suspension was used to do a cell count using a hemacytometer. Each experiment was carried out triplicate.

2.6. Endocytosis mechanism investigation

Endocytosis is known as an entry mechanism for various extracellular materials and is an energy-dependent uptake that is disturbed when cell incubation is carried out at low temperature (4 °C) [34]. Three photosensitizers were incubated with SW480 cells for 1 h at 4 °C. Then the uptake amounts were analyzed by fluorescence as described above. Sucrose (hypertonic treatment) or intracellular K^+ depletion were performed according to Hansen et al. to disrupt the formation of clathrin-coated vesicles on the cell membrane [35]. For the hypertonic treatment, SW480 cells were pre-incubated for 30 min in PBS buffer solution and supplemented with 0.45 mM sucrose before exposure to samples (TCPP nanoparticles, free TCPP and TCPP-loaded PLGA nanoparticles) for 1 h. Depletion of cytosolic K^+ was achieved by incubating SW480 cells with a K^+-free buffer solution (140 mM NaCl, 20 mM HEPES, 1 mM $CaCl_2$ and 1 mg/ml glucose, pH 6.2) for 30 min at 37 °C prior to incubation with three samples for 1 h. Treatment aimed at inhibiting caveolae-mediated endocytosis were evaluated by incubating SW480 cells with filipin at 5 μg/ml, for 30 min at 37 °C followed by incubate with three samples for 1 h. Once treatment was complete, washed three times with ice-cold PBS, and analyzed for fluorescence as described above.

2.7. Immunoblotting analysis of clathrin HC expression in cell membrane

SW480 cells with no special treatment were incubated with TCPP nanoparticles, TCPP-loaded PLGA nanoparticles and free TCPP for 1 h in the dark at 37 °C. The concentration of TCPP was 1 μM. Then cells were incubated for 30 min at 37 °C with lysis buffer (1% SDS in PBS) containing 1% protease inhibitor cocktail (Sigma Chemical Co., St. Louis, MO). After the protein concentration was measured by the BCA Protein Assay kit (Pierce Chemical, Rockford). Proteins were prepared by using 7.5% (W/V) SDS-polyacrylamide gel electrophoresis (SDS-PAGE), and the proteins were transferred to a nitrocellulose membrane. Nitrocellulose membrane was probed with a mouse monoclonal antibody against either clathrin HC (Santa Cruz Biotechnology, catalog number SC-12734, Santa Cruz, CA). Membrane was then incubated with the Anti-mouse IgG-horseradish peroxidase-conjugate (Cell Signaling Technology Inc., Beverly, MA) (1:3000 dilution) and detected by utilizing the enhanced chemiluminiscence method (ECL).

2.8. Reverse transcription-polymerase chain reaction (RT-PCR)

SW480 cells with no special treatment were then incubated with TCPP nanoparticles, TCPP-loaded PLGA nanoparticles and free TCPP for 1 h in the dark at 37 °C. Then cells were washed with ice-cold PBS and collected with trypsin digestion. Cells were treated with TRIzol® Reagent (Invitrogen Corp., Carlsbad, CA) and total RNA was obtained according to the manufacturer's direction. PCR was performed using sense (5′-C GGTTGCTCTTGTTACGG-3′) and antisense (5′-AGAGCATT AAATTTCCGGGC-3′) primers based on conserved regions of clathrin HC genes cloned from human (NM_004859). PCR conditions were as follows: 94 °C for 30 s, 52 °C for 30 s, and

70 °C for 30 s, all 30 cycles. Human house keeping gene GAPDH was used as control. GAPDH sense, 5′-AGAAGGCT GGGGCTCATTTG-3′; GAPDH antisense, 5′-AGGGGCCATC CACAGTCTTC-3′.

2.9. In vitro phototoxicity

SW480 cells were seeded into 96-well plates at 5×10^4 cells/ml (0.2 ml per well) and allowed to grow for 24 h in an incubator (5% CO_2, 37 °C, humidified atmosphere) (Jouan, France). On the day of the experiment, the culture medium was removed. A total of 200 μl of media without FCS containing TCPP nanoparticles or TCPP-loaded PLGA nanoparticles or TCPP-loaded liposomes at a final TCPP concentration of 1 μM were added to wells respectively. Cells were incubated with photosensitizers for 30 min, 45 min, 60 min, 90 min and 120 min, and then washed twice with PBS, and fresh complete medium was added. The irradiation source was a filtered Hg-arc lamp in the range of 400–440 nm at a fluence rate of 141 mW/cm^2. A light dose was approximately 15 J/cm^2. Controls were as follows: wells containing cells treated with photosensitizer but not exposed to light, cell viability was measured 24 h later by the determination of mitochondrial activity using a colorimetric 3-(4,5-Dimethylthiazol-2-yl)-2, 5-diphenyl tetrazolium bromide (MTT) assay, which ensures the capacity of mitochondrial deshydrogenase in viable cells to reduce MTT to a purple formazan precipitate. Except for the irradiation light dose, cells were protected from light.

2.10. Morphology and cell counting

SW480 cells were seeded on sterile cover glasses placed in the six-well plates, and incubated to obtain nearly confluent cell layers after 3 days. On the day of the experiment, the culture medium was removed. Media without FCS containing TCPP nanoparticles or TCPP-loaded PLGA nanoparticles at a final TCPP concentration of 1 μM were added to wells respectively. Cells were incubated for 3 h at dark. Then cells were exposed at fluences of 15 J/cm^2 for 15 min. Then cells were fixed with methanol, washed twice with PBS and stained with Hoechst 33258 staining solution according to the manufacturer's instructions (Beyotime, China). Stained nuclei were observed under a fluorescence microscope.

2.11. In vivo phototoxicity assay

Four-week-old female athymic mice (athymic *nu*/*nu*$^-$, Central South University Animal Facility; 20–22 g bw) were injected s.c. on the flank with 5×10^6 SW480 colon cancer cells in 0.2 ml of serum-free modified Eagle's medium (MEM). Animals were maintained under pathogen-free conditions. After xenografts reached about 100 mm^3 in size, the animals were randomized into five groups of four animals (four xenografts) per group to determine tumor growth rate after the following treatments: (a) control, no treatment; (b) light alone; (c) PDT, TCPP-loaded PLGA nanoparticles (1 mg/kg TCPP bw) and light exposure; (d) PDT, 1 mg/kg bw free TCPP and light exposure; and (e) PDT, 1 mg/kg bw TCPP nanoparticles and light exposure. Drugs was delivered via tail vein injection, and 48 h later a 1-cm-diameter area encompassing the tumor was irradiated (power density, 150 mW/cm^2; 400–440 nm; fluence, 120 J/cm^2) with light from a 250-mW diode laser (JENOPTIK Laserdiode GmbH Corp., Jena, Germany) coupled to a 400-mm quartz fiber-optic cable terminating in a microlens to distribute light uniformly throughout the treatment field. Growth curves representing tumor regrowth for the control and treated groups were estimated by measuring tumors in three dimensions using a caliper. Tumor volume (V) was determined by the following equation: $V = (L \times W \times H \times 0.5236)$, where L is length, W is the width, and H is the height of the xenograft (44).

2.12. Statistical analysis

The data are expressed as means ± SD. One-way analysis of variance (ANOVA) was used for statistical evaluation. A P value of <0.05 was considered significant.

3. Results

3.1. Preparation of TCPP nanoparticles and TCPP-loaded PLGA nanoparticles

Meso-tetra (carboxyphenyl) porphyrin (TCPP) nanoparticles were prepared by the method of Xianchang Gong et al. described in former paper [18]. The TCPP nanoparticles were observed with SEM (Fig. 1). The average diameter was 65 nm. The size distribution of the nanoparticles was remarkably narrow. This image was typical of those obtained for all the samples. The diameters of the nanoparticles measured by scanning electron micrograph (SEM) are 50–70 nm, which is in general agreement with the laser particle analysis result. TCPP-loaded PLGA nanoparticles were also

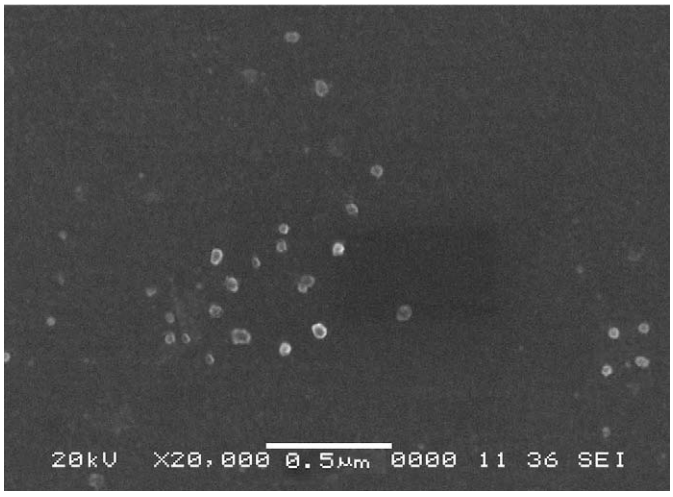

Fig. 1. (A) Scanning electron microscope (SEM) image of TCPP nanoparticles. (B) The particle size distribution of TCPP nanoparticles, average diameter = 65 nm.

prepared by the method described before [19]. The drug content and entrapment efficiency were determined spectrophotometrically at 416 nm by Hitach-4000 fluorescence spectrophotometer (Hitachi, Japan).

3.2. Colon cancer cells showed rapid uptake of TCPP nanoparticles

SW480 cellular uptake studies are shown in Fig. 2A. SW480 cells showed time-independent uptake of free TCPP and TCPP-loaded PLGA nanoparticles. The maximum uptake of these three photosensitizers happened at 3 h. Surprisingly, SW480 cells showed rapid uptake (0.0083 fmoles TCPP/cell) of TCPP nanoparticles after 1 h incubation. And the uptake level of this time point was significantly greater than the uptake of 0.0068 (TCPP-PLGA, at 2 h, $P < 0.005$) and the uptake of 0.0063 (free TCPP, at 3 h, $P < 0.005$). Also, SW480 cells showed saturation uptake of TCPP nanoparticles after 1 h incubation. As the TCPP nanoparticles uptake increasing was very hard for SW480 cells between 1 h and 3 h. And the differences of these three uptake levels (0.0083, 0.0085 and 0.0090) were not significant. For cellular uptake studies of LS174T cells and HT-29 cells, these two colon cancer cells showed the similar uptake situation with SW480 cells. They showed rapid uptake of TCPP nanoparticles after 1 h incubation, and also showed saturation uptake of TCPP nanoparticles after 1 h incubation (Fig. 2C,D). J744 macrophages showed lower uptake level of TCPP nanoparticles than other three photosensitizers after 3 h incubation (Fig. 2B). Four ethylene glycol monomethyl ether derivatives were appended to TCPP in the formation and stabilization of nanoparticles [18]. PEG chain reduced non-specific J774 macrophage uptake of TCPP nanoparticles. TCPP nanoparticles can escape from phagocytosis of reticuloendothelial system (RES).

3.3. Cellular internalization mechanism and pathway of TCPP nanoparticles, free TCPP and TCPP-loaded PLGA nanoparticles

Next, we carried out a systematic investigation of the cellular internalization mechanism and pathway of TCPP nanoparticles, free TCPP and TCPP-loaded PLGA

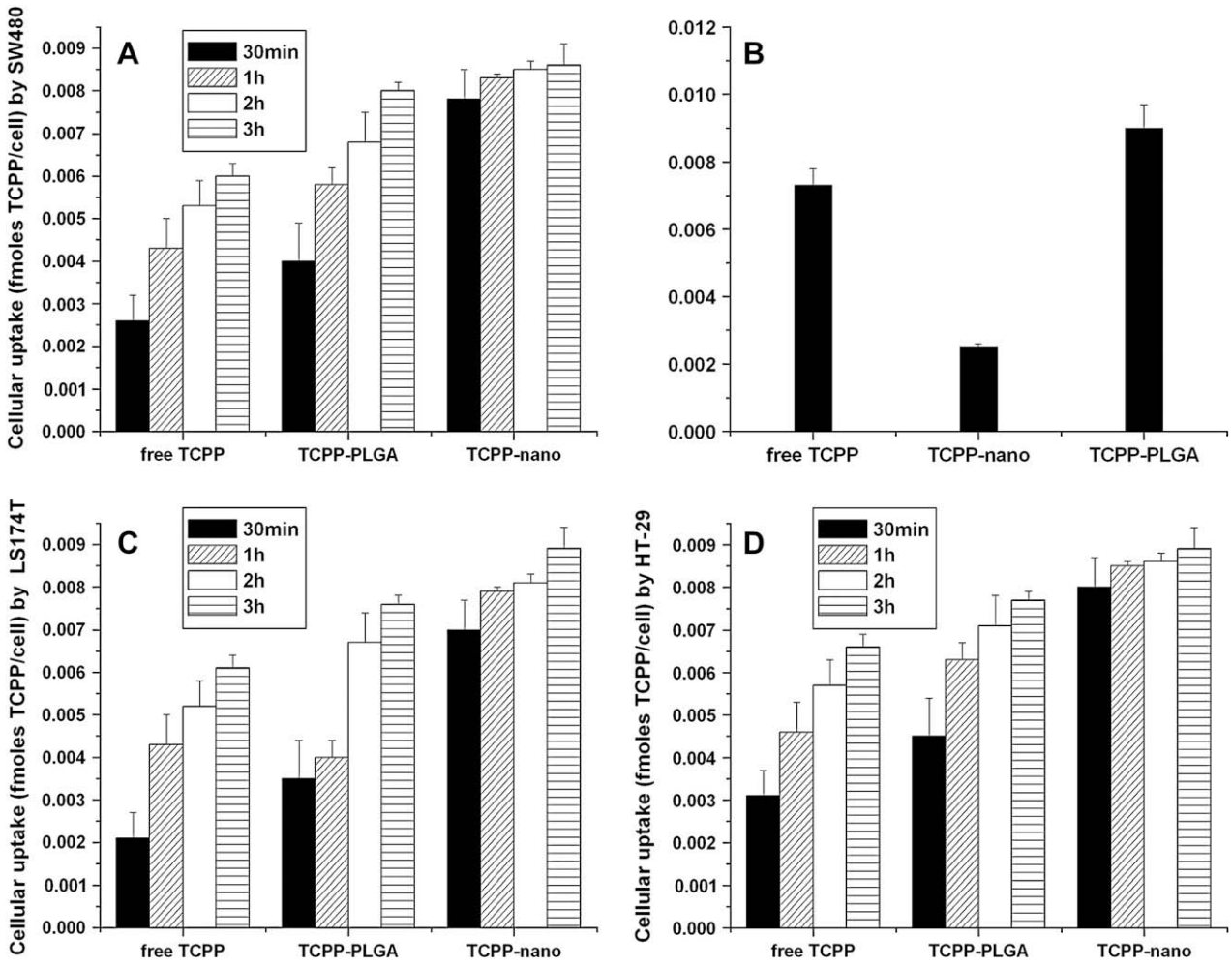

Fig. 2. (A) Cellular uptake of TCPP after SW480 cells were incubated with three photosensitizers for 30 min, 1 h, 2 h and 3 h in the dark at 37 °C. (B) Cellular uptake of TCPP after J744 macrophages were incubated with three photosensitizers for 3 h in the dark at 37 °C. (C) Cellular uptake of TCPP after LS174T cells were incubated with three photosensitizers for 30 min, 1 h, 2 h and 3 h in the dark at 37 °C. (D) Cellular uptake of TCPP after HT-29 cells were incubated with three photosensitizers for 30 min, 1 h, 2 h and 3 h in the dark at 37 °C.

nanoparticles. Endocytosis is known as an entry mechanism for various extracellular materials and is an energy-dependent uptake that is disturbed when cell incubation is carried out at low temperature (4 °C) [34]. Three photosensitizers were incubated with SW480 cells for 1 h at 4 °C. Then the uptake amounts were analyzed by fluorescence. Cellular incubations with three photosensitizers were carried out at 4 °C for 1 h. Uptake of TCPP by SW480 cells were reduced extremely. 78.3%, 73.8% and 70.7% uptake were reduced for TCPP nanoparticles, free TCPP and TCPP-loaded PLGA nanoparticles respectively at 4 °C compared to 37 °C. Researchers found that particles bind to the surfaces of phagocytes at 4 °C, but were not ingested unless the temperature of the incubation medium exceeds some critical threshold (18–21 °C) [36]. Hypertonic sucrose and K^+ depletion are known to inhibit clathrin-related processes [37,38]. These pretreatment conditions reduced cellular uptake of TCPP by 56.3% and 67.5%, respectively for TCPP nanoparticles treatment group, reduced the cellular uptake of TCPP by 34.5% and 51.7%, respectively for TCPP-loaded PLGA nanoparticles treatment group and reduced the uptake of TCPP by 30.2%, and 53.5%, respectively for free TCPP treatment group (Fig. 3). Filipin (5 μg/ml), an inhibitor of caveolae-mediated transport processes [39], did not affect TCPP uptake by the SW480 cells ($P > 0.05$) for these three photosensitizers. The results showed the uptake of these three photosensitizers by SW480 cells was a clathrin-mediated endocytosis pathway, especially TCPP nanoparticles. The inhibiting of TCPP nanoparticles internalization by these two pretreatment was more severe than other two photosensitizers. It suggested that clathrin-mediated pathway is the most important entry mechanism of TCPP nanoparticles. We observed that pretreatment of cells with filipin had no blocking effect on the cellular uptake of these tree photosensitizers (Fig. 3), which suggested little or no involvement of the caveolae-dependent cell-entry pathway for these photosensitizers. Endocytosis, the more specific of the two, can be broken down into main steps including membrane invaginations, clathrin-coated pit formation, coated pit sequestration, detachment of the newly formed vesicle via action of the small GTPase dynamin and finally movement of this new endocytic compartment away from the plasma membrane into the cytosol. These steps are extremely fast, and it is estimated that the whole cycle can occur within ≤1 min [40].

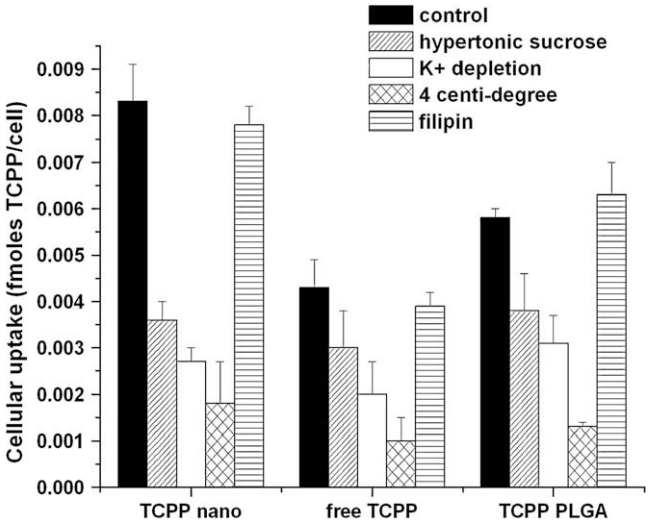

Fig. 3. Uptake of TCPP nanoparticles, free TCPP and TCPP PLGA nanoparticles by SW480 cells at 37 °C (control), at 4 °C, and at 37 °C in the presence of 0.45 mM sucrose, K^+-free buffer solution, and 5 μg/ml of filipin. Mean ± SD, $n = 3$.

3.4. Western blot analysis and RT-PCR of clathrin HC

SW480 cells with no special treatment were incubated with TCPP nanoparticles, TCPP-loaded PLGA nanoparticles and free TCPP for 1 h in the dark at 37 °C. To verify the existence of clathrin HC and analyze the expression difference at protein and mRNA level of the treated cells, Western blot analysis and RT-PCR were performed. In Fig. 4, the results showed that clathrin HC antibody detected a 180 kDa-size protein in SW480 cells treated with TCPP nanoparticles, free TCPP and TCPP-loaded PLGA nanoparticles. RT-PCR results also detected 744 bp products in SW480 cells treated with these three photosensitizers. These results further confirmed that the uptake of these photosensitizers was a clathrin-mediated endocytosis pathway. Clathrin HC protein and mRNA expressions were strongly elevated by incubating with TCPP nanoparticles after 1 h (Fig. 4A,C). The clathrin HC protein expression level of TCPP nanoparticles treatment group was significantly higher than the level of free TCPP group ($P < 0.005$), and also higher than the level of TCPP-loaded PLGA nanoparticles group ($P < 0.005$) (Fig. 4B). Densitometry analysis of RT-PCR products showed the mRNA level of TCPP nanoparticles group was higher than the level of free TCPP group ($P < 0.005$), and also higher than the level of TCPP-loaded PLGA nanoparticles group ($P < 0.005$) (Fig. 4D). Elevated levels of intracellular TCPP are associated with increased expression of clathrin HC. These results might explain why TCPP nanoparticles were internalized by SW480 cells so rapidly. Researchers' findings indicated that endocytosis of PLGA nanoparticles in rabbit conjunctival epithelial cells occurred through multiple mechanisms, out of which clathrin-coated pits might not contribute significantly. Internalization of PLGA nanoparticles by epithelial cells may be a process similar to adsorptive endocytosis [26]. This was the reason why the TCPP-loaded PLGA nanoparticles uptake by SW480 cells was partly reduced by incubating with clathrin inhibitors. It has been shown previously that materials >1 μm in size generally have difficulty undergoing endocytotic cellular uptake, even at 37 °C [41]. The clathrin lattice, which forms the outside of a coated vesicle, can have an outside diameter ranging from ≥600 Å to ≥2000 Å [40]. Free TCPP can easily form aggregates as large-size micro-particles (>1 μm) as free TCPP show low aqueous stability. Agglomeration of free TCPP in water may affect the clathrin-coated vesicles assembly and closure around the large-size microparticles. It may reduce the efficiency of clathrin-coated

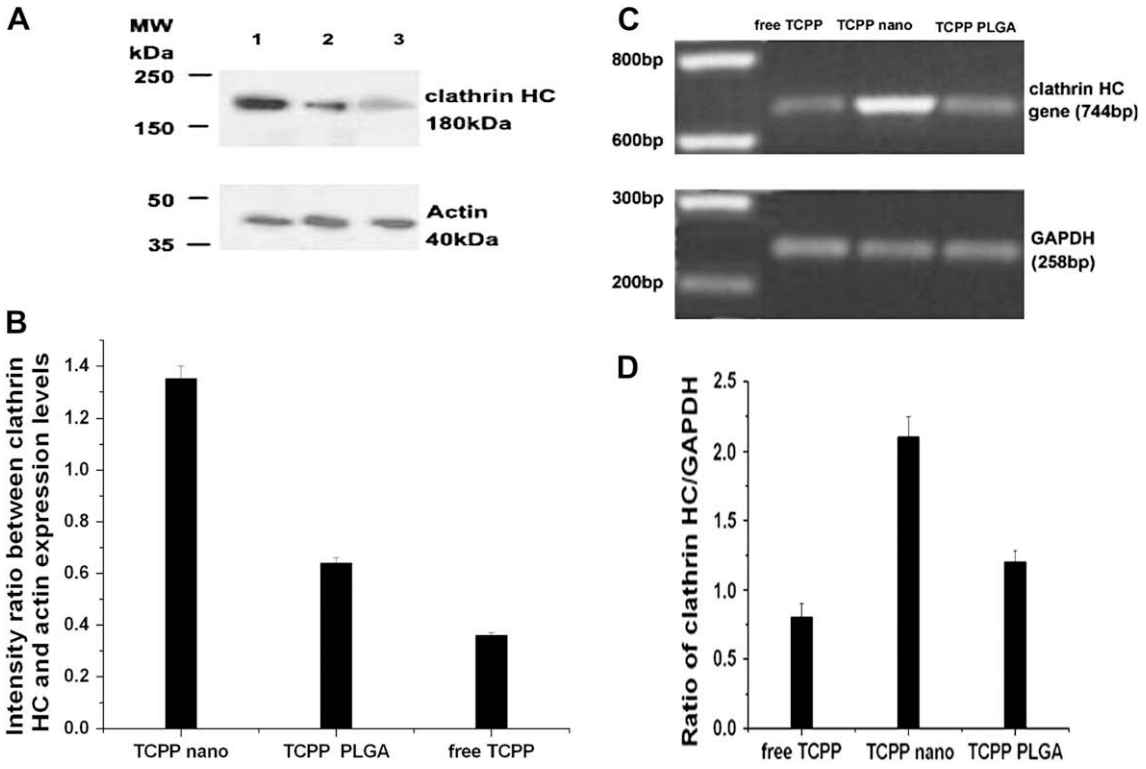

Fig. 4. (A) Western blot analysis and (C) RT-PCR analysis of clathrin HC expression of SW480 cells exposed to TCPP nanoparticles (1), TCPP PLGA nanoparticles (2) and frees TCPP (3) for 1 h in the dark at 37 °C. (B) Quantitative analysis of clathrin HC protein expression normalized against actin protein expression. Ratio = mean ± SD ($n = 4$). (D) RT-PCR signal levels for clathrin HC expression. The data are expressed as a ratio of clathrin HC signal to GAPDH expression. Ratio = mean ± SD ($n = 4$).

vesicle endocytosis. But TCPP nanoparticles can be easily captured by vesicles as TCPP nanoparticles show large surface area to adsorb on surface of cell membrane efficiently. Cargo (TCPP nanoparticles) recruitment accompanied with bilayer vesiculation can also finish rapidly. Above-mentioned factors led to rapid and efficient uptake of TCPP nanoparticles.

3.5. Cell viability after incubating with photosensitizers and irradiation

After irradiation at a dose of 15 J/cm^2, cell viability decreased when the incubation time increased for TCPP-loaded PLGA nanoparticles, and free TCPP. But this change was not significant for TCPP nanoparticles from 30 min to 120 min ($P > 0.05$) (Fig. 5). Also, TCPP nanoparticles showed very high photocytotoxic effect to SW480 cells after short incubation time (23%, 30 min) (Fig. 5). A total of 39% and 25% of survival fractions were obtained with free TCPP and TCPP-loaded PLGA nanoparticles at 120 min, while TCPP nanoparticles yielded only 23% of cell viability even at 30 min. The results showed TCPP nanoparticles produce the highest photocytotoxic effect. The effect was related with the results that SW480 cells showed rapid and saturation uptake of TCPP nanoparticles only after 1 h incubation, and TCPP nanoparticles with no polymer coating had large surface area to produce toxic singlet oxygen by reacting with dioxygen. But, TCPP-loaded PLGA nanoparticles must need to release drug TCPP from the core in order to react with dioxygen in cells. It demonstrated that this photosensitizer (TCPP) with a range of photonic properties did not need to be prepared by encapsulation in matrices or by designed self-assembly

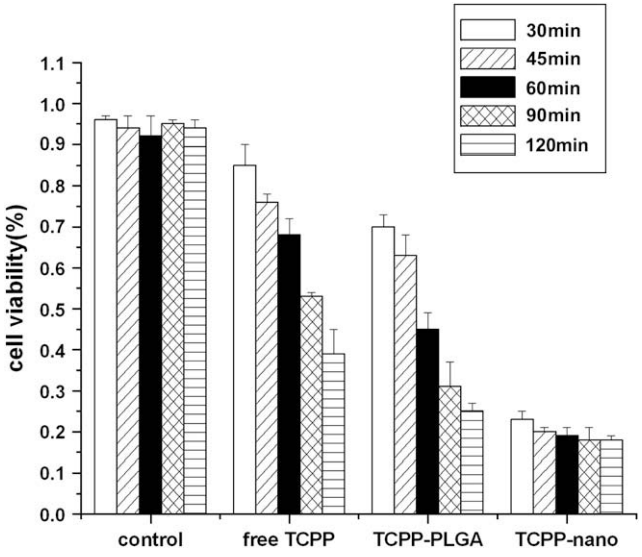

Fig. 5. MTT assay of SW480 cells after irradiation (15 J/cm^2). Before irradiation, SW480 Cells were incubated with three photosensitizers (free TCPP, TCPP-loaded PLGA nanoparticles and TCPP nanoparticles) for 30 min, 45 min, 60 min, 90 min and 120 min.

a priori. The matrix may severely limit the functionality of the particles in the former case [18]. Results obtained from former study demonstrated that the photocytotoxicity of meso-tetra (hydroxyphenyl) porphyrin (p-THPP) PLGA nanoparticle against EMT-6 cells showed time-delayed effects appearing at 18 h post-irradiation [33]. Though the cell damage resulting to photochemical reactions are not immediately lethal, the drug release time delayed the photocytotoxicity function. Coated-vesicle which carries a lot of cargo (TCPP nanoparticles) detachment from plasma membranes, and this process requires the GTPase-containing protein dynamin. Clathrin-uncoating activity happens in the cytoplasm stimulated by Hsp70 proteins which can target the J domain of clathrin coated-vesicle [42,43]. The cargo is released in cytosol. The released TCPP nanoparticles were reacted with dioxygen after exposed to special wavelength light.

3.6. Analysis of apoptotic cells after photodynamic treatment

When stained with H-33258, characteristic morphological changes were found in photosensitized cells by incubation with TCPP nanoparticles, TCPP-loaded PLGA nanoparticles or free TCPP at a final TCPP concentration of 1 μM for 1 h. Analyses of nuclear morphology by H-33258 are shown in Fig. 6. A great amount of apoptotic cells (53%) were obtained analyzing the cells after photodynamic treatments with 15 J/cm^2 of irradiation for TCPP nanoparticles treatment group (Fig. 6D). Apoptotic cell death was predominant in all photosensitizers' treatment groups. The percentage of apoptotic cells in all cells for TCPP-loaded PLGA nanoparticles and free TCPP groups were 21% and 9% respectively (Fig. 6E). In addition to apoptotic cells, the remaining

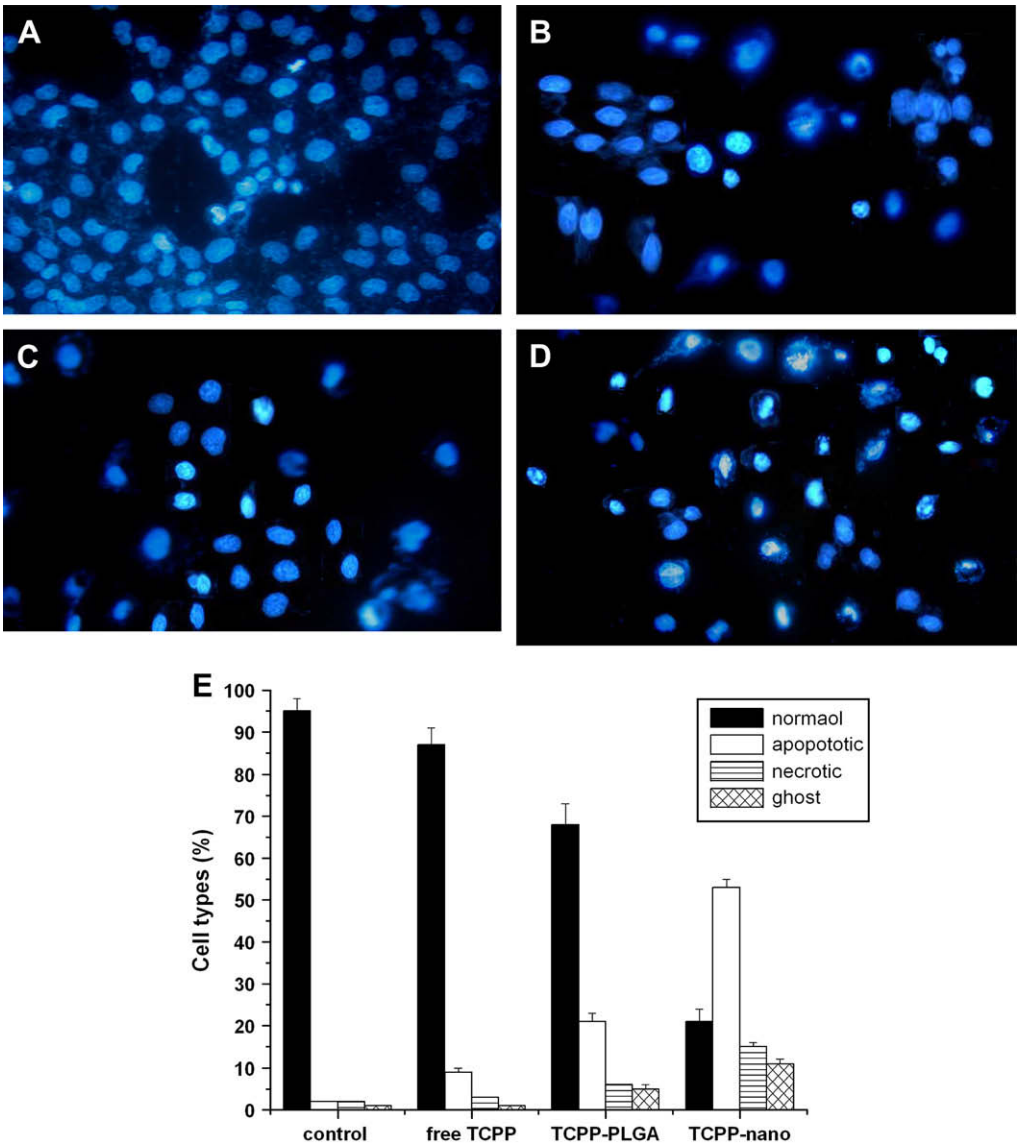

Fig. 6. Fluorescence photomicrographs of SW480 cells stained with H-33258. (A) Untreated cells. (B) Cells treated with free TCPP (1 μM) and 15 J/cm^2 of illumination. (C) Cells treated with TCPP (1 μM)-loaded PLGA nanoparticles and 15 J/cm^2 of illumination. (D) Cells treated with TCPP (1 μM) nanoparticles and 15 J/cm^2 of illumination.

population corresponded to necrotic and ghost cells. Photographic characteristics of normal cells are observed in Fig. 6A.

3.7. Growth Inhibition of SW480 xenografts by photosensitizers-PDT

The PDT effects after receiving 1 mg/kg of free TCPP, TCPP-loaded PLGA nanoparticles and TCPP nanoparticles are shown in Fig. 7. After implantation of SW480 cells, tumors in the control animals continued to increase. Neither the light nor the untreated resulted in any gross effects on the tumors. The mean tumor sizes at the end of the study for light only group and untreated group were $710 \pm 59\ mm^3$ and $750 \pm 50\ mm^3$, respectively (mean $\pm$ S.D.; $n = 4$). Tumor growth was significantly delayed when PDT with TCPP nanoparticles was done. The TCPP nanoparticles plus PDT group demonstrated the most dramatic efficacy: the final mean tumor load was $135 \pm 19\ mm^3$ (mean $\pm$ S.D. $n = 4$, 24 days). On the other hand, free TCPP ($350 \pm 49\ mm^3$, 24 days) and TCPP-loaded PLGA nanoparticles ($250 \pm 43\ mm^3$, 24 days) resulted in a less reducing effect compared to TCPP nanoparticles. After 1 day PDT treatment, the mean tumor size of TCPP nanoparticles treated group ($15 \pm 2\ mm^3$) was reduced significantly.

4. Discussion and conclusion

Carbohydrate conjugated porphyrins with a 2 nm diameter and an 8 nm bilayer thickness have showed great potential in developing commercialized drugs for photodynamic therapy. They have great water solubility than most naturally occurring and synthetic, *meso* substituted, porphyrins. This property can not only increase the efficacy of drug delivery but also assist the drug elimination from the organism after treatment.

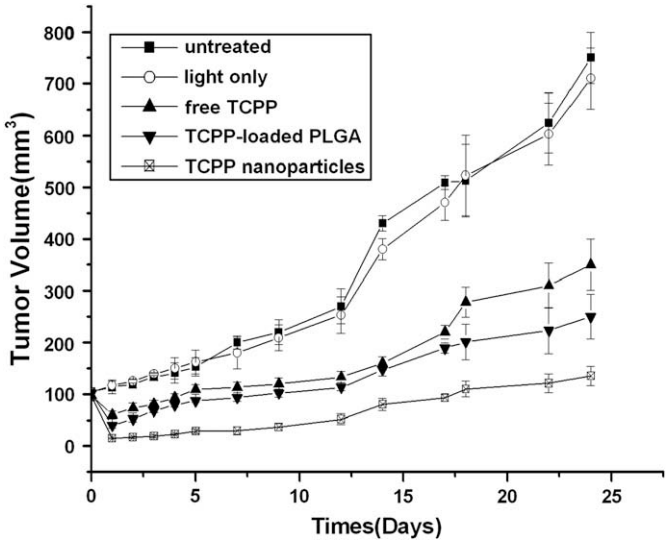

Fig. 7. Effect of TCPP-PDT on SW480 xenografts. SW480 xenografts were either untreated or treated with light alone, free TCPP-PDT, TCPP nanoparticles-PDT and TCPP-loaded PLGA nanoparticles-PDT. Tumor volumes were measured as described in Section 2 The data represent the mean $\pm$ S.D. of the volumes of four xenografts in each arm.

Furthermore, Carbohydrate conjugated porphyrins can have specific interactions with proteins on cell membranes and thus exhibit specific targeting of cancer cells [32]. Photocytotoxicity experiments of X. Chen and C.M. Drain [32] showed an increase in the photocytotoxicity among the four *meso*-tris (*para*-glucosylphenyl) porphyrins bearing mono (*n*-undecyl), mono (*n*-butyl), monophenyl and mono (pentafluorophenyl) derivatives in KB cells correlated with the increasing hydrophilicity. *Meso*-tris (*para*-glucosylphenyl) mono (pentafluorophenyl) porphyrin is the most active photodamaging agent among the 16 tested glycosylated porphyrins.

Porphyrin nanoparticles stability was assayed by both DLS and UV-vis over time on batches of nanoparticles stored as they were made in closed vials in the dark in air. Preparation experiments conditions were found that resulted in porphyrin nanoparticles colloids that were stable for at least a month for a range of substituted macrocycles. Many preparations are stable for more than a year. The nanoparticle solutions can be diluted and somewhat concentrated, but cannot be dried as this leads to irreversible agglomeration. An inter-nanoparticle material exchange assay was designed to examine the stability of porphyrinic nanoparticles in the presence of other porphyrinic nanoparticles. This is expected because of the PEG stabilizer and the water of hydration inhibit interactions between the particles and prevent agglomeration and precipitation [44].

Experiments of our research indicated that clathrin-mediated pathway is the most important entry mechanism of TCPP nanoparticles. Colon cancer cells (SW480 cells, HT-29 cells and LS174T cells) showed saturation uptake of TCPP nanoparticles after 1 h incubation. We think colon cancer cells intake a lot of porphyrin nanoparticles by clathrin-mediated pathway. This saturated uptake of nanoparticles by colon cancer cells induced the high photocytotoxicity *in vitro* and *in vivo*. Results from our *in vitro* and *in vivo* studies indicated that TCPP nanoparticles are a novel promising photosensitizer for colon cancer treatment. Porphyrin nanoparticles-based PDT may be considered as potential therapy in the PDT therapy. However, a lot of laboratory studies are needed before taking it into clinical practices, such as biodistribution, skin photosensitivity, drug release profile and pharmacokinetics. While continuing to explore more in the chemistry, future investigation of the lead compounds should be carried out in localization of the porphyrin nanoparticles within the cell, drug release profile, the pharmacokinetics and possibly biological effects on animal models.

This is the first report about the use of a special photosensitizer: TCPP nanoparticles for photodynamic therapy. In this study, we prepared TCPP nanoparticles with no matrix cover. We found that this nano-sized photosensitizer was internalized by SW480 cells by a clathrin-mediated pathway and led to rapid and saturate uptake of this photosensitizer. As a result, this special photosensitizer showed very high photocytotoxic effect on SW480 cells. The *in vivo* tumor growth inhibition experiment indicated that TCPP nanoparticles plus PDT treatment induced the most dramatic tumor-inhibiting efficacy in all TCPP treated groups.

Acknowledgements

This work was supported by the National High Technology Research and Development Project of China (No. 2002AA216011) and the Major State Basic Research Development Program of China (No.2004CB518802).

References

[1] Ideta R, et al. Nanotechnology-based photodynamic therapy for neovascular disease using a supramolecular nanocarrier loaded with a dendritic photosensitizer. Nano Lett 2005;5(12):2426–31.
[2] Goff BA, et al. Treatment of ovarian cancer with photodynamic therapy and immunoconjugates in a murine ovarian cancer model. Br J Cancer 1996;74(8):1194–8.
[3] Soukos NS, et al. Epidermal growth factor receptor-targeted immunophotodiagnosis and photoimmunotherapy of oral precancer in vivo. Cancer Res 2001;61(11):4490–6.
[4] Konan YN, Gurny R, Allemann E. State of the art in the delivery of photosensitizers for photodynamic therapy. J Photochem Photobiol B 2002;66(2):89–106.
[5] Peterson CM, et al. Combination chemotherapy and photodynamic therapy with N-(2-hydroxypropyl) methacrylamide copolymer-bound anticancer drugs inhibit human ovarian carcinoma heterotransplanted in nude mice. Cancer Res 1996;56(17):3980–5.
[6] Leroux J, et al. N-isopropylacrylamide copolymers for the preparation of pH-sensitive liposomes and polymeric micelles. J Control Release 2001; 72(1-3):71–84.
[7] Polo L, et al. The effect of different liposomal formulations on the interaction of Zn (II)-phthalocyanine with isolated low and high density lipoproteins. Int J Biochem Cell Biol 1995;27(12):1249–55.
[8] Akhlynina TV, et al. Nuclear targeting of chlorin e6 enhances its photosensitizing activity. J Biol Chem 1997;272(33):20328–31.
[9] Bisland SK, Singh D, Gariepy J. Potentiation of chlorin e6 photodynamic activity in vitro with peptide-based intracellular vehicles. Bioconjug Chem 1999;10(6):982–92.
[10] Lu ZR, Kopeckova P, Kopecek J. Polymerizable Fab′ antibody fragments for targeting of anticancer drugs. Nat Biotechnol 1999;17(11):1101–4.
[11] Kongshaug M, et al. Binding of drugs to human plasma proteins, exemplified by Sn(IV)-etiopurpurin dichloride delivered in cremophor and DMSO. Int J Biochem 1993;25(5):739–60.
[12] Woodburn K, Kessel D. The alteration of plasma lipoproteins by cremophor EL. J Photochem Photobiol B 1994;22(3):197–201.
[13] Dye D, Watkins J. Suspected anaphylactic reaction to Cremophor EL. Br Med J 1980;280(6228):1353.
[14] Michaud LB. Methods for preventing reactions secondary to Cremophor EL. Ann Pharmacother 1997;31(11):1402–4.
[15] Damoiseau X, et al. Increase of the photosensitizing efficiency of the Bacteriochlorin a by liposome-incorporation. J Photochem Photobiol B 2001;60(1):50–60.
[16] Isele U, et al. Pharmacokinetics and body distribution of liposomal zinc phthalocyanine in tumor-bearing mice: influence of aggregation state, particle size, and composition. J Pharm Sci 1995;84(2):166–73.
[17] Dillon J, et al. In vitro and in vivo protection against phototoxic side effects of photodynamic therapy by radioprotective agents WR-2721 and WR-77913. Photochem Photobiol 1988;48(2):235–8.
[18] Gong X, et al. Preparation and characterization of porphyrin nanoparticles. J Am Chem Soc 2002;124(48):14290–1.
[19] Marsh M, McMahon HT. The structural era of endocytosis. Science 1999;285(5425):215–20.
[20] Bondi ML, et al. Novel cationic solid-lipid nanoparticles as non-viral vectors for gene delivery. J Drug Target 2007;15(4):295–301.
[21] Ebbesen M, Jensen TG. Nanomedicine: techniques, potentials, and ethical implications. J Biomed Biotechnol 2006;2006(5):51516.
[22] Panyam J, Labhasetwar V. Biodegradable nanoparticles for drug and gene delivery to cells and tissue. Adv Drug Deliv Rev 2003;55(3):329–47.
[23] Davda J, Labhasetwar V. Characterization of nanoparticle uptake by endothelial cells. Int J Pharm 2002;233(1-2):51–9.
[24] Missirlis D, et al. Doxorubicin encapsulation and diffusional release from stable, polymeric, hydrogel nanoparticles. Eur J Pharm Sci 2006;29(2): 120–9.
[25] Park JS, et al. N-acetyl histidine-conjugated glycol chitosan self-assembled nanoparticles for intracytoplasmic delivery of drugs: endocytosis, exocytosis and drug release. J Control Release 2006;115(1):37–45.
[26] Qaddoumi MG, et al. Clathrin and caveolin-1 expression in primary pigmented rabbit conjunctival epithelial cells: role in PLGA nanoparticle endocytosis. Mol Vis 2003;9:559–68.
[27] Qaddoumi MG, et al. The characteristics and mechanisms of uptake of PLGA nanoparticles in rabbit conjunctival epithelial cell layers. Pharm Res 2004;21(4):641–8.
[28] Huang M, et al. Uptake of FITC-chitosan nanoparticles by A549 cells. Pharm Res 2002;19(10):1488–94.
[29] Panyam J, Labhasetwar V. Dynamics of endocytosis and exocytosis of poly(D,L-lactide-co-glycolide) nanoparticles in vascular smooth muscle cells. Pharm Res 2003;20(2):212–20.
[30] Panyam J, et al. Rapid endo-lysosomal escape of poly(DL-lactide-co-glycolide) nanoparticles: implications for drug and gene delivery. Faseb J 2002;16(10):1217–26.
[31] Foster KA, Yazdanian M, Audus KL. Microparticulate uptake mechanisms of in-vitro cell culture models of the respiratory epithelium. J Pharm Pharmacol 2001;53(1):57–66.
[32] Leng X, et al. Assembling a mixed phthalocyanine-porphyrin array in aqueous media through host-guest interactions. Org Lett 2007;9(2):231–4.
[33] Konan YN, et al. Encapsulation of p-THPP into nanoparticles: cellular uptake, subcellular localization and effect of serum on photodynamic activity. Photochem Photobiol 2003;77(6):638–44.
[34] de Figueiredo RC, Soares MJ. Low temperature blocks fluid-phase pinocytosis and receptor-mediated endocytosis in *Trypanosoma cruzi* epimastigotes. Parasitol Res 2000;86(5):413–8.
[35] Hansen SH, Sandvig K, van Deurs B. Clathrin and HA2 adaptors: effects of potassium depletion, hypertonic medium, and cytosol acidification. J Cell Biol 1993;121(1):61–72.
[36] Saito N, et al. Biodegradable poly-D,L-lactic acid-polyethylene glycol block copolymers as a BMP delivery system for inducing bone. J Bone Joint Surg Am 2001;83-A(Suppl. 1(Pt 2)):S92–8.
[37] Lutz W, Kumar R. Hypertonic sucrose treatment enhances second messenger accumulation in vasopressin-sensitive cells. Am J Physiol 1993;264(2 Pt 2):F228–33.
[38] Madshus IH, et al. Effect of reduced endocytosis induced by hypotonic shock and potassium depletion on the infection of Hep 2 cells by picornaviruses. J Cell Physiol 1987;131(1):14–22.
[39] Orlandi PA, Fishman PH. Filipin-dependent inhibition of cholera toxin: evidence for toxin internalization and activation through caveolae-like domains. J Cell Biol 1998;141(4):905–15.
[40] Kirchhausen T. Clathrin. Annu Rev Biochem 2000;69:699–727.
[41] Rejman J, et al. Size-dependent internalization of particles via the pathways of clathrin- and caveolae-mediated endocytosis. Biochem J 2004;377(Pt 1):159–69.
[42] Schlossman DM, et al. An enzyme that removes clathrin coats: purification of an uncoating ATPase. J Cell Biol 1984;99(2):723–33.
[43] Ungewickell E, et al. Role of auxilin in uncoating clathrin-coated vesicles. Nature 1995;378(6557):632–5.
[44] Iyer AK, et al. High-loading nanosized micelles of copoly(styrene-maleic acid)-zinc protoporphyrin for targeted delivery of a potent heme oxygenase inhibitor. Biomaterials 2007;28(10):1871–81.